# Experimental Characterization of Collapse-Mode CMUT Operation

Ömer Oralkan, *Member, IEEE*, Baris Bayram, *Student Member, IEEE*, Goksen G. Yaralioglu, *Member, IEEE*, A. Sanli Ergun, *Member, IEEE*, Mario Kupnik, David T. Yeh, *Student Member, IEEE*, Ira O. Wygant, *Student Member, IEEE*, and Butrus T. Khuri-Yakub, *Fellow, IEEE*

***Abstract*—This paper reports on the experimental characterization of collapse-mode operation of capacitive micromachined ultrasonic transducers (CMUTs). CMUTs are conventionally operated by applying a direct current (DC) bias voltage less than the collapse voltage of the membrane, so that the membrane is deflected toward the bottom electrode. In the conventional regime, there is no contact between the membrane and the substrate; the maximum alternating current (AC) displacement occurs at the center of the membrane. In collapse-mode operation, the DC bias voltage is first increased beyond the collapse voltage, then reduced without releasing the collapsed membrane. In collapse-mode operation, the center of the membrane is always in contact with the substrate. In the case of a circular membrane, the maximum AC displacement occurs along the ring formed between the center and the edge of the membrane.**

**The experimental characterization presented in this paper includes impedance measurements in air, pulse-echo experiments in immersion, and one-way optical displacement measurements in immersion for both conventional and collapse-mode operations. A 205-$\mu$m $\times$ 205-$\mu$m 2-D CMUT array element composed of circular silicon nitride membranes is used in the experiments. In pulse-echo experiments, a custom integrated circuit (IC) comprising a pulse driver, a transmit/receive switch, a wideband low-noise preamplifier, and a line driver is used. By reducing the parasitic capacitance, the use of a custom IC enables pulse-echo measurements at high frequencies with a very small transducer. By comparing frequency response and efficiency of the transducer in conventional and collapse regimes, experimental results show that a collapsed membrane can be used to generate and detect ultrasound more efficiently than a membrane operated in the conventional mode. Furthermore, the center frequency of the collapsed membrane can be changed by varying the applied DC voltage. In this study, the center frequency of a collapsed transducer in immersion is shown to vary from 20 MHz to 28 MHz with applied DC bias; the same transducer operates at 10 MHz in the conventional mode. In conventional mode, the maximum peak-to-peak pressure is 370 kPa on the transducer surface for a 40-ns, 25-V unipolar pulse excitation. In collapse mode, a 25-ns, 25-V unipolar pulse generates 590 kPa pressure at the surface of the transducer.**

Manuscript received July 9, 2005; accepted February 27, 2006. This work was supported by the United States Office of Naval Research under grant N00014-02-1-0007, and National Institutes of Health under grants CA99059 and HL67647.

The authors are with the Edward L. Ginzton Laboratory, Stanford University, Stanford, CA 94305-4088 (e-mail: ooralkan@stanford.edu).

## I. Introduction

Capacitive micromachined ultrasonic transducers (CMUTs) are in the process of moving from research studies to mainstream applications. Significant progress in CMUTs has been demonstrated since the first introduction of this technology in the early 1990s. Moving from the first functional device in 1993 [1] to first full-scale, phased-array imaging results in 2001 [2] took less than 10 years. Industry leaders in the field of ultrasonic imaging have expressed great interest in this young, but rapidly progressing, transducer technology. Commercial scanners using one-dimensional (1-D) CMUT arrays recently have produced clinical-quality images [3]–[5].

Advantages in underlying fabrication techniques make CMUTs an attractive option for use in next-generation imaging systems. CMUT technology uses integrated circuit (IC) processing techniques to fabricate arrays of ultrasonic transducers in different forms and sizes. Basic microlithography and batch processing techniques allow thousands of arrays to be fabricated at once on each production run. Arrays with different operating frequencies, different numbers of elements, and even different geometries can be fabricated on a single silicon wafer, resulting in both uniform quality and reduced cost. Batch manufacturing provides significant cost reduction compared to existing piezoelectric transducer fabrication technology, which relies on meticulous and labor-intensive steps, such as hand lapping, polishing, and high-precision dicing. CMUT technology also conveniently integrates the transducer array with supporting electronic circuits (either monolithically [6], [7] or in a flip-chip package [8]).

In addition, a thin membrane can be built with the same planar fabrication techniques above a submicron sealed cavity—crucial to obtain high electric fields for improved transducer performance. Because CMUTs are inherently wideband, fractional bandwidths in excess of 100% can be achieved easily with no additional complexity in the process. CMUTs also demonstrate sensitivity comparable to piezoelectric transducers, but over a much larger frequency range [9].

CMUTs are designed to generate high acoustic output power using low-voltage pulses, a specification that is especially critical for integration of transducer arrays

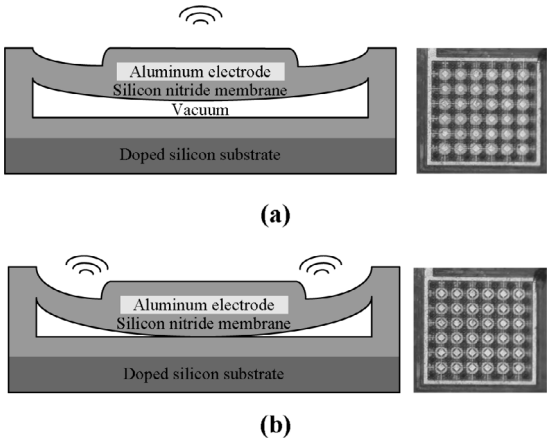


Fig. 1. Schematic representations (left) and micrographs (right) of CMUTs in (a) conventional and (b) collapse-mode operations.

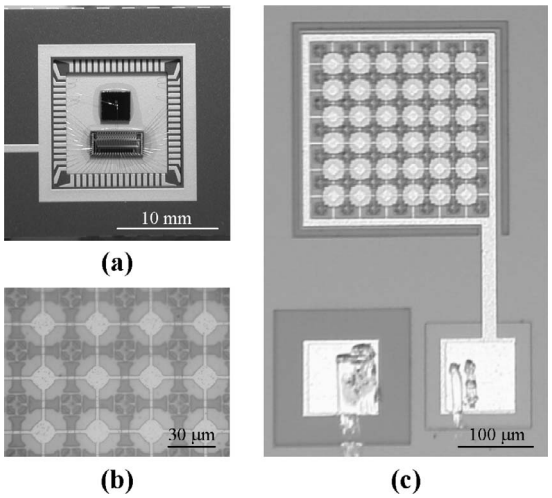


Fig. 2. CMUT element used in this study. (a) CMUT wire-bonded to the front-end IC for pulse-echo measurements. (b) Magnified view of CMUT cells. (c) Magnified view of the CMUT element.

with electronic circuits. In order to improve operation speed, power consumption, and functionality, semiconductor devices used in integrated circuits have been scaled to smaller and smaller sizes. To prevent reliability problems due to high electric field intensities, supply voltages must be scaled down as well. This trend toward reducing device size makes it more difficult to obtain high-voltage pulses from mainstream integrated circuits, and it increases the importance of new operating regimes that produce more acoustic output pressure for the given electrical pulse amplitude dictated by the IC technology.

This paper demonstrates experimentally that a CMUT in collapse mode could be used to generate and detect ultrasound more efficiently than a CMUT in conventional mode of operation. The frequency characteristics of CMUTs also are considerably different in the collapse-mode operation regime. Because of different frequency characteristics, this new way of operating CMUTs also extends design and operating flexibility.

This paper presents the first collapse-mode operation results in the 10–28 MHz frequency range. An integrated front-end circuit enabled measurements at such high frequencies.

Section II of this paper describes different operation regimes for CMUTs, focusing on the collapse-mode operation. Section III explains the experimental methods used in this study. Section IV presents the experimental results. Section V provides a brief intuitive explanation for collapse-mode operation, and it addresses reliability issues.

## II. Collapse-Mode Operation of CMUTs

Three different CMUT operating regimes have been reported so far: conventional, collapse, and collapse-snapback. In the conventional operation, the CMUT is biased at a voltage close to the collapse voltage. The sum of the DC bias and the AC excitation are adjusted so that the membrane does not make contact with the substrate. The DC bias causes a deflection in the membrane, and induces stress within the membrane to balance the electrostatic attraction. Driving the membrane with an AC voltage superimposed on the DC bias voltage generates ultrasound. If the biased membrane is subjected to ultrasound, a current output is generated by the capacitance change under constant bias voltage. The amplitude of this output current is a function of the frequency of the incident wave, the bias voltage, and the capacitance of the device. In this mode, the maximum AC displacement occurs at the center of the membrane. A schematic representation of the conventional operation is shown in Fig. 1(a).

Collapse and snapback are two important physical phenomena associated with the CMUT membrane. As the bias voltage on the CMUT is increased, the electrostatic force gradient reaches a point at which it is greater than the mechanical force gradient, and the membrane collapses onto the bottom electrode. This instability observed in electrostatically deflected elastic systems also is known as the "pull-in" instability. The calculation of the collapse voltage was previously described [10]. After collapse, when the bias voltage is decreased to a certain "snapback" voltage, which is lower than the collapse voltage, the membrane snaps back. Snapback describes the quick motion of the membrane when it loses contact with the substrate and recovers its shape and position at that voltage prior to collapse.

For collapse-mode operation, the DC bias must be set to a value larger than this snapback voltage, so that the center of the membrane will be in contact with the bottom electrode at all times. The insulating layer on the bottom electrode prevents any short circuit that might occur if the membrane material were conducting (and also acts as an etch stop for the sacrificial layer process). As in conventional operation, an AC voltage is applied in collapse mode to generate ultrasound. In the collapse-mode operation, the maximum AC displacement occurs along the ring formed between the center and the edges of the membrane

[Fig. 1(b)]. A micrograph of the CMUT in both conventional and collapse modes are also shown in Fig. 1 along with schematic descriptions. The dark region surrounding the top electrode in Fig. 1(b) shows that the midportion of the membrane is in contact with the substrate. Finite-element analysis (FEA) has revealed that a CMUT operating in the collapsed regime (between collapse and snapback voltages) has a coupling efficiency ($k_T^2$) higher than a CMUT operating in the conventional regime below its collapse voltage [11]. Preliminary experimental results on collapse-mode operation at low frequencies were presented previously [12]. This paper presents experimental results in high frequency ranges to support previous theoretical findings and to investigate the frequency characteristics of a CMUT operating in these conventional and collapse regimes.

In the collapse-snapback operating regime for CMUTs, the DC bias voltage on the CMUT is set at a value between collapse and snapback voltages. A sufficiently large bipolar voltage swing first collapses the membrane then releases it, creating a total displacement that can be as large as the total gap height. This operating regime was recently characterized experimentally [13].

Using finite-element methods, the performance of a CMUT in these three different operating regimes was studied in [14]; this paper concluded that collapse-mode operation provides more output pressure and is more linear than conventional mode. The collapse-snapback operation generates the highest acoustic output, but it also is the most nonlinear. This last operating regime is perhaps most suitable for transmit-only use, such as ultrasonic ablation and other therapeutic applications.

TABLE I
PHYSICAL PARAMETERS OF THE 2-D CMUT ARRAY ELEMENT.

| | |
|---|---|
| Size of an element, $\mu$m $\times$ $\mu$m | $205 \times 205$ |
| Number of cells per element | 36 |
| Cell radius ($r_{cell}$), $\mu$m | 15 |
| Metal electrode radius ($r_{el}$), $\mu$m | 7.5 |
| Center-to-center cell spacing ($d_{cell}$), $\mu$m | 35 |
| Membrane thickness above the electrode ($t_{m1}$), $\mu$m | 0.30 |
| Sandwiched metal electrode thickness ($t_e$), $\mu$m | 0.30 |
| Membrane thickness below the electrode ($t_{m2}$), $\mu$m | 0.31 |
| Gap thickness ($t_g$), $\mu$m | 0.12 |
| Insulating layer thickness ($t_i$), $\mu$m | 0.29 |
| Silicon substrate thickness, $\mu$m | 500 |

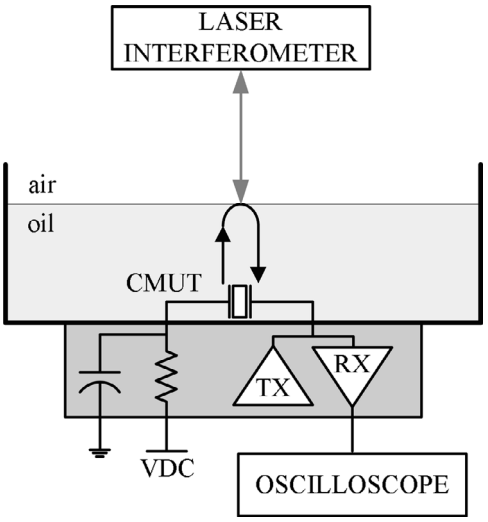


Fig. 3. A schematic of the experimental setup.

## III. Experimental Methods

In order to characterize the transducer operation in conventional and collapse regimes, the electrical input impedance of a CMUT is measured in air. Pulse-echo tests are performed in immersion by using a simple setup comprised of a CMUT and a custom designed front-end IC that facilitates high signal quality in the measurements. Optical displacement measurements, alongside pulse-echo measurements, assess the transmit-only performance of the CMUT during both conventional and collapse-mode operations.

The CMUT used in this study is a stand-alone, 2-D array element, fabricated using silicon surface micromachining. The membrane material is silicon nitride with a half-metalized electrode sandwiched in the middle of the membrane. Part of the membrane beneath the metal electrode was deposited by using a low-pressure, chemical-vapor deposition process (LPCVD), whereas the part above the electrode was deposited by using plasma-enhanced, chemical-vapor deposition (PECVD). Burying the electrode in the membrane decreases the effective gap height, increases the device capacitance, and decreases the collapse voltage [15]. This configuration also provides a protective coating for the top electrode. Physical dimensions of this transducer are summarized in Table I. A micrograph of the transducer is shown in Fig. 2(c).

A high-frequency probe (model ACP 40-W, Cascade Microtech Inc., Beaverton, OR) was used to access the electrodes of the CMUT to measure impedance. The electrical input impedance of the transducer was measured in air using a vector network analyzer (model 8751A, Hewlett-Packard Co., Palo Alto, CA). The device capacitance values and the resonant frequency in air were extracted from the impedance measurements.

The experimental setup for pulse-echo tests consists of a transmit/receive (T/R) IC connected to the CMUT. The T/R IC used in this experiment includes 16-channel T/R circuits, each consisting of a pulse driver, a T/R switch, a wideband low-noise preamplifier, and an output buffer to drive off-chip loads. Although all 16 channels can be used in parallel, in the experiments described here, only one channel is connected to the CMUT. The preamplifier has a transimpedance gain of 25 k$\Omega$. The one-channel preamplifier-output buffer combination dissipates 25 mW from a 5-V supply. For a CMUT with 2-pF total capacitance, the transducer-preamplifier combination yields a 3 dB bandwidth greater than 30 MHz, and the pulse driver

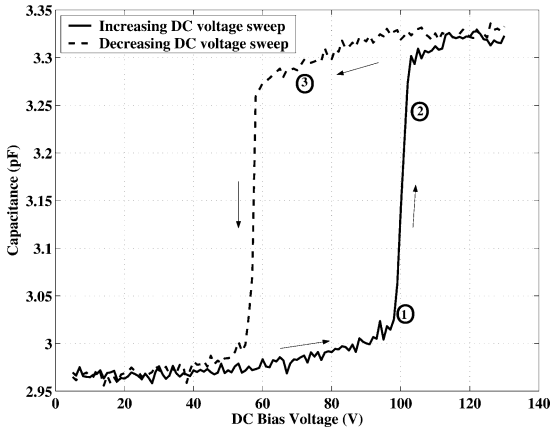


Fig. 4. Measured capacitance as a function of DC bias voltage. Region 1: conventional, region 2: collapse, region 3: presnapback.

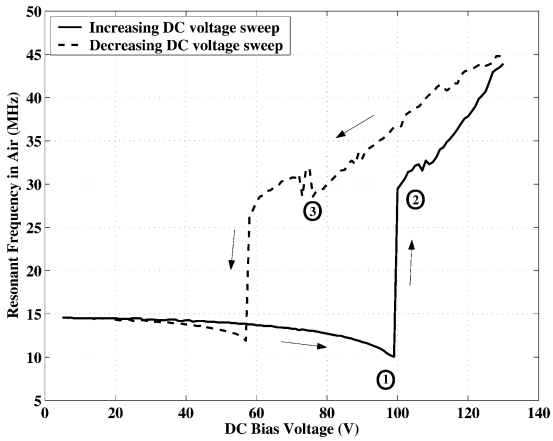


Fig. 5. Measured resonant frequency in air as a function of DC bias voltage. Region 1: conventional, region 2: collapse, region 3: presnapback.

generates a 25-V rectangular pulse as narrow as 15 ns. The output buffer can drive a 50-Ohm transmission line with a 1-V peak-to-peak signal with no distortion in the specified frequency range. The T/R switch isolates the receiver input from the transducer during the transmit cycle, and it connects the receiver to the transducer during the receive cycle (while isolating the pulse driver). The T/R circuits were fabricated in a two-metal, high-voltage, analog bipolar-CMOS (BiCMOS) process.

The CMUT was placed in the cavity of a standard 64-pin, dual-in-line (DIP-64) package, along with the T/R IC. Wire bonding provided the electrical connections between the CMUT, the T/R IC, and the package pins. A photograph of the package is shown in Fig. 2(a). The CMUT was immersed in vegetable oil. The oil-air interface was 2 mm away from the transducer, as shown in Fig. 3. The transducer was biased using a high-voltage DC power supply (model PS310 Stanford Research Systems, Inc., Sunnyvale, CA). A 25-V, unipolar pulse with varying width was used for excitation. The received echo signals were sampled at a rate of 1 GSa/s, and digitized with 8-bit resolution by a digitizing oscilloscope (model 54825A, Hewlett-Packard Co., Palo Alto, CA). The digitized waveforms were recorded while sweeping the DC bias voltage. For both impedance measurements and pulse-echo tests, the DC bias voltage was first increased in the positive direction, then reduced back to the starting voltage.

A laser interferometer (model OFV-511, Polytec GmbH, Waldbronn, Germany) was used to measure the displacement of the air-oil interface. The interferometer was connected to an ultrasonics vibrometer controller OFV-2700/2 (Polytec) that contains a modified wideband displacement decoder OVD-30-30-PI (Polytec) with a frequency range extending from 50 kHz to 30 MHz, and sensitivity in the subnanometer range. Standard version of the decoder has a bandwidth of 20 MHz, and the customized version used in this study has a 30 MHz bandwidth. The manufacturer confirmed the accuracy of the system from 50 kHz to 30 MHz with maximum additional error of +1.5 dB/−3 dB in the amplitude frequency response (flatness). The specified displacement range for this system is ±50 nm. The displacement is measured in the oil-air interface so that the total transmit response of the transducer can be measured at a single location. The measurement of the displacement on the transducer surface requires a complete area scan and a numeric integration of the resulting displacement data to obtain the total output of the transducer element. Therefore, the measurement at the oil-air interface is more convenient.

## IV. Experimental Results

This section presents the experimental results on CMUTs operated in conventional and collapsed regimes, focusing on the behavior of CMUTs as a function of the DC bias. The results and the analysis presented here are based on the electrical input impedance measurements in air, the amplitude and frequency measurements of the first reflection from the oil-air interface in the pulse-echo tests, and the optical interferometric displacement measurements at the oil-air interface.

The change in capacitance (at 70 MHz) and the resonant frequency of the CMUT in air were extracted by measuring the electrical input impedance. Fig. 4 shows the change in the measured capacitance as a function of the DC bias voltage for both increasing and decreasing voltage sweeps relative to the measured capacitance at zero bias. Because of the increasing deflection at the center of the membrane, the capacitance increases with the increasing DC bias voltage. At 98 V, the device capacitance increases by 0.05 pF, which corresponds approximately to one-sixth of the simulated device capacitance (0.32 pF). At about 100 V, the membrane collapses and the capacitance jumps up another 0.3 pF, resulting in a total change of 0.35 pF, relative to the zero-bias condition. Further increase in the bias voltage does not cause any significant increase in the capacitance. When the DC bias voltage is lowered, the capacitance slowly decreases; after a 0.05 pF decrease, the membrane snaps back, and the capacitance slowly returns

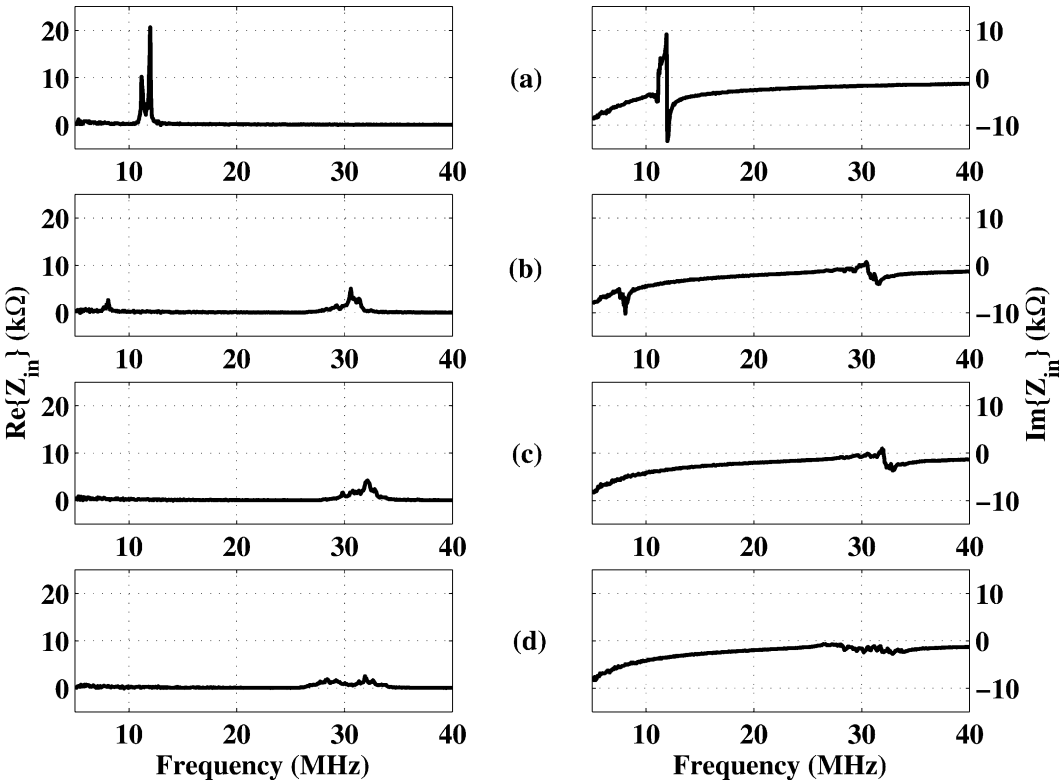


Fig. 6. Real and imaginary parts of the input impedance: (a) conventional regime, $V_{DC} = 98$ V; (b) transition from conventional to collapsed regime, $V_{DC} = 101$ V; (c) collapsed regime, $V_{DC} = 103$ V; (d) collapsed regime prior to snapback, $V_{DC} = 75$ V. The real part of the impedance is shown in the left panel; the imaginary part of the impedance is shown in the right panel.

to its initial value during the increasing sweep. The capacitance curve shown in Fig. 4 includes the parasitic capacitance of the impedance measurement system.

The regions marked as 1, 2, and 3 on the C-V curve (Fig. 4) represent measurements for conventional, collapsed, and presnapback regions, respectively. These same regions also are used consistently for pulse-echo measurements.

The resonant frequency, defined as the frequency at which the real part of the input impedance is maximum, is measured in air as a function of DC bias voltage (Fig. 5). In the conventional regime, when the bias voltage increases from zero to 100 V, the resonant frequency decreases from 15 MHz to 10 MHz. This decrease in resonant frequency is attributed to the effects of spring softening [16]. At collapse, with increasing DC voltage, the resonant frequency first jumps to 30 MHz, then shifts to 45 MHz. Because the width of the ring-shaped membrane increases, when the membrane is slowly released after collapse, the resonant frequency slowly decreases. At snapback, the resonant frequency drops back to 13 MHz.

The real and imaginary parts of the electrical input impedance for conventional, collapse, and conventional-to-collapse transition regimes are shown in Fig. 6. The observation of both low-frequency and high-frequency resonances during the transition from one regime to another is due to nonuniformity among the cells, a result of the fabrication process. For example, during the increasing sweep, at about 100 V, some cells collapse but others do not, creating two different resonances. However, the difference in the collapse voltages of cells is no more than a few volts; as a result, a sharp transition from conventional to collapse-mode can be observed.

In addition to measuring input impedance in air, conventional and collapse-mode operation also were characterized in immersion, using pulse-echo tests. The excitation pulse width of 20 ns was chosen to capture the frequency response of the device under test up to 50 MHz. Fig. 7 shows the received peak-to-peak echo amplitude as a function of the DC bias voltage. During the increasing sweep of the DC bias voltage, the received echo amplitude increased with increasing bias voltage, as demonstrated earlier [9]. During the increasing DC voltage sweep, the membrane collapsed at 100 V. The hysteresis seen in capacitance and resonant frequency measurements also is shown in Fig. 7 in a slightly different fashion; as the DC bias voltage was lowered, the received echo amplitude first increased, then again reached the values observed during the increasing sweep when the membrane snapped back. Fig. 7 suggests that the snapback occurred at about 55 V. To eliminate the effects of frequency-dependent attenuation and the diffraction, and the excitation pulse shape, Fig. 8 shows the maxima of the corrected pulse-echo frequency spectra as a function of DC bias voltage.

This experimental observation (shown in Figs. 7 and 8) is in line with recently reported theoretical expectations

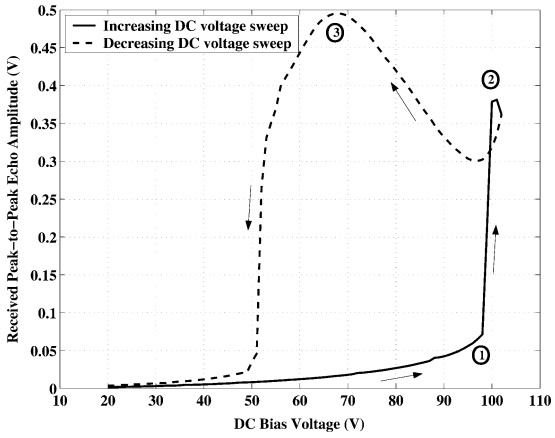


Fig. 7. Received peak-to-peak echo amplitude as a function of the DC bias voltage. Region 1: conventional, region 2: collapse, region 3: presnapback.

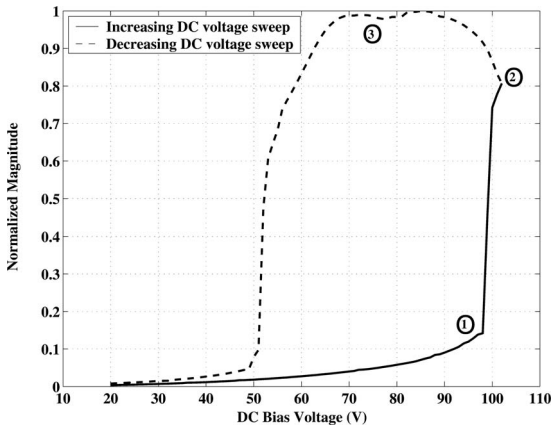


Fig. 8. Maxima of the corrected pulse-echo frequency spectra as a function of DC bias voltage. The compensation includes frequency dependent, two-way diffraction and attenuation losses, and the frequency spectrum of the transmit pulse. Region 1: conventional, region 2: collapse, region 3: presnapback.

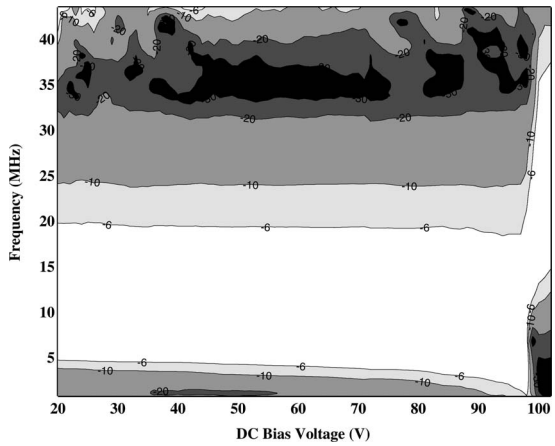


Fig. 9. A contour plot of the normalized frequency response as a function of increasing DC bias voltages.

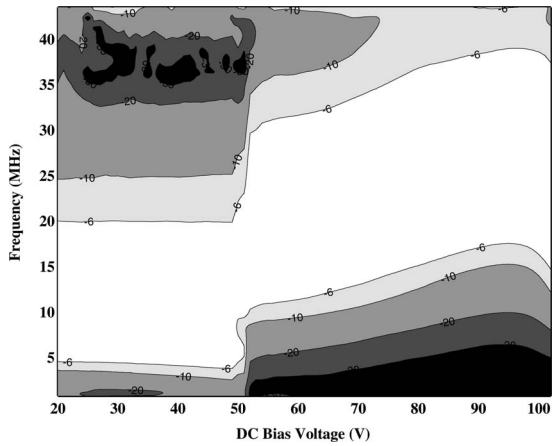


Fig. 10. A contour plot of the normalized frequency response as a function of decreasing DC bias voltages.

[11], which showed that coupling efficiency increases following the collapse as the bias voltage is lowered. In addition to the static analysis presented in [11], recent dynamic analysis results also show that collapse mode provides a higher average output pressure at a higher frequency compared to conventional mode of operation [17], [18].

The change in frequency response as a function of the DC bias voltage sweep also was investigated in our experiments. After compensating for two-way attenuation and diffraction losses, and the transmit pulse shape, the Fourier transform of the first echo signal is used to assess the pulse-echo frequency spectrum of the CMUT front-end. Fig. 9 displays the normalized frequency spectrum for the increasing sweep at different DC bias points. Contour lines −6 dB, −20 dB, and −30 dB are shown in the figure. Similarly, Fig. 10 displays the normalized frequency spectrum for the decreasing sweep at different DC bias points. These plots show that the frequency response shifts to higher frequencies after the collapse, and it stays at those high frequencies during the decreasing sweep—before the membrane snaps back. Figs. 11 and 12 show the measured center frequency and the −6 dB bandwidth, respectively, for both increasing and decreasing DC bias voltage sweeps. In the conventional regime, the center frequency moves from 12 MHz at 20 V to 10 MHz at 98 V due to a spring-softening effect. After collapse and during the decreasing DC bias voltage sweep, the center frequency shifts from 28 MHz at 95 V to 20 MHz at 55 V. At snapback, the center frequency returns to its original value in the conventional regime. The fractional bandwidth was calculated using data presented in Figs. 11 and 12. For clarity, fractional bandwidth as a function of DC bias voltage is shown in Fig. 13. In Fig. 13, it is observed that the fractional bandwidth in conventional mode changes from 120% to 180%, and the fractional bandwidth is about 80–90% in collapse mode. The frequency shift observed in these experiments is in line with the dynamic analysis results presented in [17].

As mentioned above, in the pulse-echo experiments described so far, a 20-ns, 25-V unipolar pulse excitation was used to obtain the frequency response of the CMUT. In an

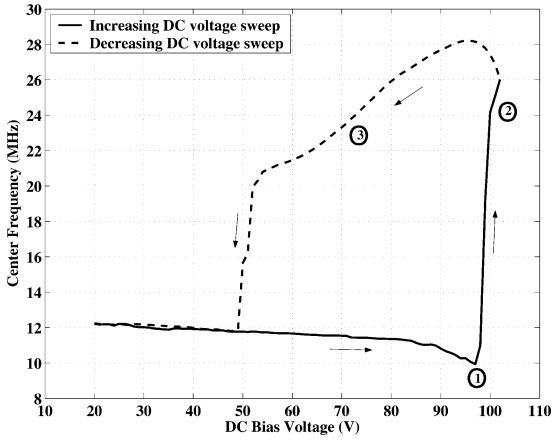


Fig. 11. Center frequency of the CMUT front end as a function of the DC bias voltage. Region 1: conventional, region 2: collapse, region 3: presnapback.

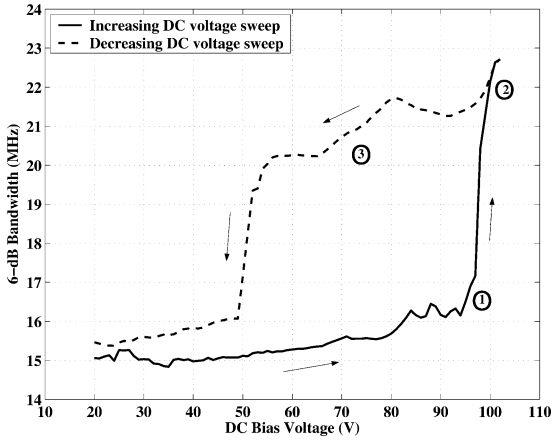


Fig. 12. A 6 dB bandwidth of the CMUT front end as a function of the DC bias voltage. Region 1: conventional, region 2: collapse, region 3: presnapback.

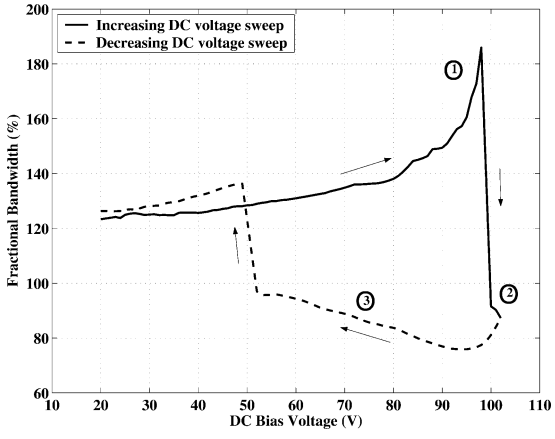


Fig. 13. Fractional bandwidth of the CMUT front end as a function of the DC bias voltage. Region 1: conventional, region 2: collapse, region 3: presnapback.

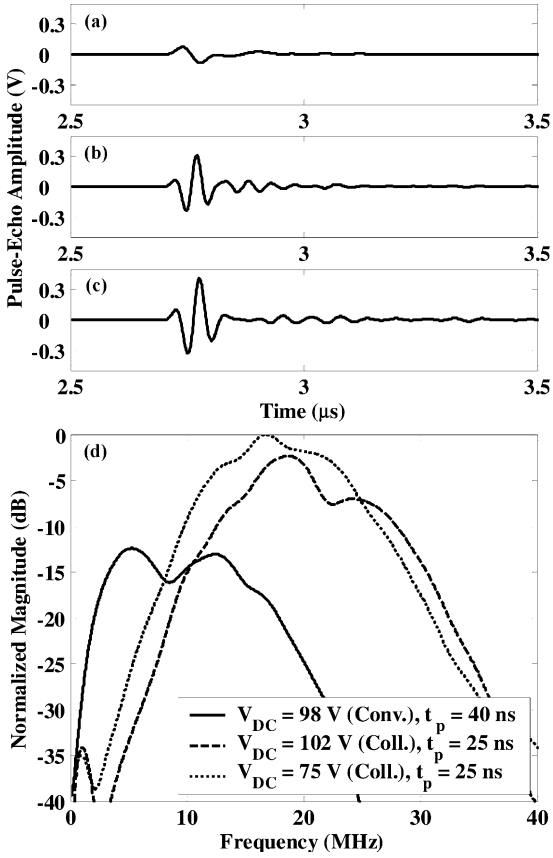


Fig. 14. Pulse-echo results. (a) Received echo signal ($V_{DC}$ = 98 V (conventional), $t_p$ = 40 ns). (b) Received echo signal ($V_{DC}$ = 102 V (collapse mode), $t_p$ = 25 ns). (c) Received echo signal ($V_{DC}$ = 75 V (collapse mode), $t_p$ = 25 ns). (d) Corresponding frequency transforms.

imaging application, however, the total pulse-echo performance can be optimized by using different pulse widths for conventional and collapsed regimes. In this experiment, we determined that a 40-ns pulse maximizes the echo amplitude for conventional operation of this particular device; 25-ns pulse width is optimal for collapse mode operation. Fig. 14 shows the received echo signals in conventional, collapsed, and presnapback regimes, when the transducer was excited by 40-ns, 25-ns, and 25-ns pulses, respectively.

Displacement measurements at the oil-air interface (obtained by a laser interferometer) facilitate the transmit-only characterization of the device in both conventional and collapse-mode operations. The displacement waveforms were recorded simultaneously with the pulse-echo waveforms. The displacement of the air-oil interface was divided by two to take the interface reflection into account. The pressure waveforms are obtained by calculating the time derivative of the displacement data, and multiplying the result by the acoustic impedance of the medium.

The peak-to-peak pressure measured at the oil-air interface as a function of the DC bias voltage is shown in Fig. 15. The maximum peak-to-peak pressure in collapse mode is measured as 70 kPa, which is approximately three times larger than the maximum pressure in conventional mode. The same ratio in the pulse-echo measure-

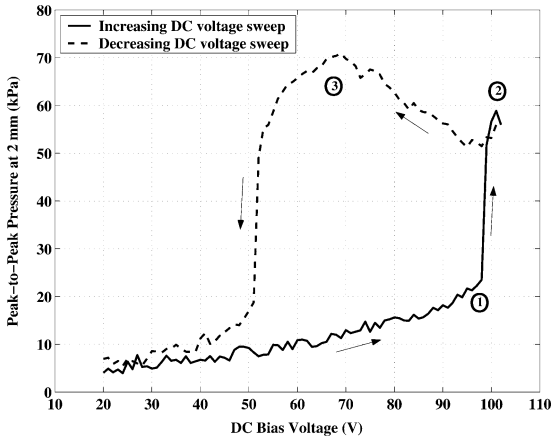


Fig. 15. Peak-to-peak pressure at the oil-air interface as a function of the DC bias voltage. Region 1: conventional, region 2: collapse, region 3: presnapback.

ments shown in Fig. 7 is seven, indicating that the collapse mode improves both transmit and receive performances. For a fully reciprocal system, the two-way improvement should be the square of the one-way improvement. In the experimental system described here, the transmitter's output impedance and the receiver's input impedance are not identical, which violates full reciprocity. However, the results described here clearly show that collapse-mode operation improves not only the output pressure but also the receive sensitivity of the CMUT.

The pressure waveforms measured at the oil-air interface (Fig. 16) are in good agreement with the corresponding pulse-echo measurements presented in Fig. 14. Similar to the pulse-echo case, to eliminate the effects of frequency dependent attenuation and the diffraction, and the excitation pulse shape, Fig. 17 shows the maxima of the corrected one-way transmit frequency spectra as a function of DC bias voltage. In conventional mode, the maximum peak-to-peak pressure is 370 kPa on the transducer surface for a 40-ns, 25-V unipolar pulse excitation. In collapse mode, a 25-ns, 25-V unipolar pulse generates 590 kPa pressure at the surface of the transducer.

## V. Discussion

This section provides a brief intuitive explanation for collapse-mode operation, and it addresses several reliability issues.

The improved performance of CMUTs in collapsed regime can be explained intuitively by considering the equivalent circuit model. The efficiency of CMUTs is determined by the electromechanical transformer ratio, expressed as the product of the device capacitance and the electric field strength across the gap beneath the membrane. A collapsed membrane with a small contact in the middle has effectively a fraction of the gap of a noncollapsed membrane. This reduced gap increases both the electric field and the capacitance per unit area, resulting in an improved electromechanical transformer ratio.

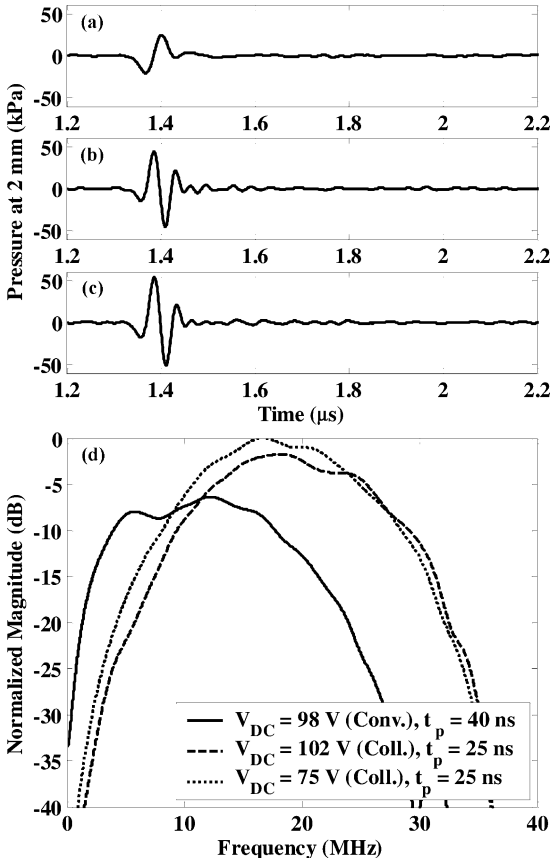


Fig. 16. Laser interferometer measurements. (a) Pressure at the oil-air interface ($V_{DC} = 98$ V (conventional), $t_p = 40$ ns). (b) Pressure at the oil-air interface ($V_{DC} = 102$ V (collapse mode), $t_p = 25$ ns). (c) Pressure at the oil-air interface ($V_{DC} = 75$ V (collapse mode), $t_p = 25$ ns). (d) Corresponding Fourier transforms.

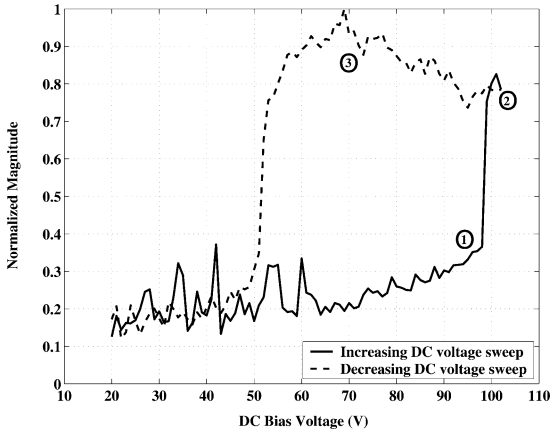


Fig. 17. Maxima of the corrected, one-way transmit frequency spectra as a function of DC bias voltage. The compensation includes frequency-dependent, one-way diffraction and attenuation losses, and the frequency spectrum of the transmit pulse. Region 1: conventional, region 2: collapse, region 3: presnapback.

The frequency shift in the collapsed regime is caused by the shape of the membrane. In the conventional operation, the moving part of the membrane is a complete circle, with maximum displacement at the center. In the collapsed regime, the moving part of the membrane is an annular ring. The larger the contact area, the narrower the ring; hence, the operating frequency is higher.

The description of collapse-mode operation of CMUTs usually raises questions about reliability. In general, early failure of microelectromechanical devices is caused by defects introduced during fabrication, shock, electrostatic discharge, frictional wear, material fatigue, creep, dielectric breakdown of thin films, charge buildup, and stiction [19]. In this study, no destructive failure was observed during the experiments, in which a DC bias as high as 130 V was used along with a 25-V pulse excitation. The dielectric layers in the device are sufficiently thick that the electric field is less than the intrinsic breakdown field strength. Good film quality prevents defect-related extrinsic breakdown.

However, the snapback voltage as experimentally measured in this study was about 30 V lower than expected. Despite this discrepancy between the experimental and the expected snapback voltage, all measurements were repeatable for the device presented here. Possible reasons for the shift in the snapback voltage include charge buildup in the nitride films [20] and the presence of other strong intermolecular (adhesive) forces [21].

When the membrane is in contact with the insulating layer, a charge can build up in the nitride [20]. The polarity of the charges on the membrane and on the insulating layer are opposite, thus attracting more of the membrane and increasing the capacitance of the system. This charge buildup also can cause the snapback voltage to shift to lower voltages. A fixed charge in the dielectric layers appears as a voltage offset, resulting in a shift in the C-V curve along the voltage axis. This contact-charging phenomenon has been extensively investigated for capacitive microelectromechanical RF switches [22], [23]. A CMUT design using isolation posts as a solution to charging problems also was introduced recently [24].

After snapback, the measured echo amplitude for the same bias voltages is only slightly greater than the amplitude during the increasing sweep, suggesting that the charge accumulation is not the only reason for low snapback voltage. Similarly, in collapse mode, CMUT exhibits a higher resonant frequency in air during the decreasing sweep compared to the increasing sweep, indicating that the membrane cannot be released easily. When the surfaces of the membrane and the substrate make contact, or come into proximity, strong intermolecular (adhesive) forces may exist [21]. The strength of these adhesive forces will depend on the roughness of the surfaces in contact, with a stronger pull-off force for smoother surfaces. The snapback voltage of the CMUT will be reduced in the presence of these attractive forces.

The long-term reliability of CMUTs operating in collapse mode is subject to ongoing research. Although charging and stiction do not cause immediate catastrophic failure, they can affect the device performance over time, and thus require stringent operating conditions. Therefore, the physical phenomena behind the snapback voltage shift should be well understood.

## VI. Conclusions

This paper presents a detailed experimental characterization of the collapse-mode operation of CMUTs in both air and immersion. An experimental integrated ultrasound front-end, including a CMUT and a custom-designed T/R IC, was used for pulse-echo measurements in immersion.

The experimental results obtained in this study suggest that a collapsed membrane can be used to generate and detect ultrasound more efficiently than the conventional mode of operation. This collapse-mode operation of CMUTs not only improves the coupling efficiency, but also offers the additional design and operating flexibility of tuning the frequency and bandwidth by changing the DC bias voltage. CMUTs can be designed to operate in the collapsed state, so that target frequency characteristics can be met in this collapse regime. Additional operating flexibility might include a dual-mode navigational imaging system that normally provides a coarse resolution and switches to fine resolution on demand.

In light of the results presented here, it seems that the collapse-mode operation is a viable technique to improve the acoustic output and receive sensitivity of CMUTs. Devices used in this study were originally designed for use in a conventional regime. Further theoretical understanding of this operation is necessary to develop a model for transducers designed specifically for collapse-mode operation. Also as a future experiment, two CMUTs designed and optimized to operate at the same frequency range—one in conventional and the other in the collapse mode—can be compared to each other.

## Acknowledgments

The authors thank National Semiconductor Corporation, Bill Broach, and the Portable Power group for their support in circuit design and for providing the custom integrated circuits, and Tim Brand for dicing the transducers. David Yeh is supported by a National Defense Science and Engineering Graduate Fellowship. Mario Kupnik acknowledges the FWF Austrian Science Fund for financial support.

## References

[1] M. I. Haller and B. T. Khuri-Yakub, "A surface micromachined electrostatic ultrasonic air transducer," in *Proc. IEEE Ultrason. Symp.*, 1994, pp. 1241–1244.

[2] Ö. Oralkan, A. S. Ergun, J. A. Johnson, M. Karaman, U. Demirci, K. Kaviani, T. H. Lee, and B. T. Khuri-Yakub, "Capacitive micromachined ultrasonic transducers: Next-generation

arrays for acoustic imaging?," *IEEE Trans. Ultrason., Ferroelect., Freq. Contr.*, vol. 49, pp. 1596–1610, Nov. 2002.

[3] D. M. Mills and L. S. Smith, "Real-time in-vivo imaging with capacitive micromachined ultrasound transducer (cMUT) linear arrays," in *Proc. IEEE Ultrason. Symp.*, 2003, pp. 568–571.

[4] D. M. Mills, "Medical imaging with capacitive micromachined ultrasound transducer (cMUT) arrays," in *Proc. IEEE Ultrason. Symp.*, 2004, pp. 384–390.

[5] G. Caliano, R. Carotenuto, E. Cianci, V. Foglietti, A. Caronti, and M. Pappalardo, "A cMUT linear array used as echographic probe: Fabrication, characterization, and images," in *Proc. IEEE Ultrason. Symp.*, 2004, pp. 395–398.

[6] R. A. Noble, R. R. Davies, M. M. Day, L. Koker, D. O. King, K. M. Brunson, A. R. D. Jones, J. S. McIntosh, D. A. Hutchins, T. J. Robertson, and P. Saul, "A cost-effective and manufacturable route to the fabrication of high-density 2D micromachined ultrasonic transducer arrays and (CMOS) signal conditioning electronics on the same silicon substrate," in *Proc. IEEE Ultrason. Symp.*, 2001, pp. 941–944.

[7] C. Daft, S. Calmes, D. deGraca, K. Patel, P. Wagner, and I. Ladabaum, "Microfabricated ultrasonic transducers monolithically integrated with high voltage electronics," in *Proc. IEEE Ultrason. Symp.*, 2004, pp. 493–496.

[8] I. O. Wygant, D. T. Yeh, X. Zhuang, A. Nikoozadeh, Ö. Oralkan, A. S. Ergun, M. Karaman, and B. T. Khuri-Yakub, "A miniature real-time volumetric ultrasonic imaging system," in *Proc. SPIE Med. Imag. Conf.*, 2004, pp. 26–36.

[9] Ö. Oralkan, X. C. Jin, F. L. Degertekin, and B. T. Khuri-Yakub, "Simulation and experimental characterization of a 2-D capacitive micromachined ultrasonic transducer array element," *IEEE Trans. Ultrason., Ferroelect., Freq. Contr.*, vol. 46, pp. 1337–1340, Nov. 1999.

[10] A. Nikoozadeh, B. Bayram, G. G. Yaralioglu, and B. T. Khuri-Yakub, "Analytical calculation of collapse voltage of cMUT membrane," in *Proc. IEEE Ultrason. Symp.*, 2004, pp. 256–259.

[11] B. Bayram, E. Hæggström, G. G. Yaralioglu, and B. T. Khuri-Yakub, "A new regime for operating capacitive micromachined ultrasonic transducers," *IEEE Trans. Ultrason., Ferroelect., Freq. Contr.*, vol. 50, pp. 1184–1190, Sep. 2003.

[12] Y. Huang, E. Hæggström, B. Bayram, X. Zhuang, A. S. Ergun, C. H. Cheng, and B. T. Khuri-Yakub, "Collapsed regime operation of capacitive micromachined ultrasonic transducers based on wafer-bonding technique," in *Proc. IEEE Ultrason. Symp.*, 2003, pp. 1161–1164.

[13] B. Bayram, Ö. Oralkan, A. S. Ergun, E. Hæggström, G. G. Yaralioglu, and B. T. Khuri-Yakub, "Capacitive micromachined ultrasonic transducer design for high power transmission," *IEEE Trans. Ultrason., Ferroelect., Freq. Contr.*, vol. 52, no. 2, pp. 326–339, Feb. 2005.

[14] B. Bayram, E. Hæggström, A. S. Ergun, G. G. Yaralioglu, and B. T. Khuri-Yakub, "Dynamic analysis of CMUTs in different regimes of operation," in *Proc. IEEE Ultrason. Symp.*, 2003, pp. 481–484.

[15] G. G. Yaralioglu, A. S. Ergun, B. Bayram, E. Hæggström, and B. T. Khuri-Yakub, "Calculation and measurement of electromechanical coupling coefficient of capacitive micromachined ultrasonic transducers," *IEEE Trans. Ultrason., Ferroelect., Freq. Contr.*, vol. 50, no. 4, pp. 449–456, Apr. 2003.

[16] I. Ladabaum, X. C. Jin, H. T. Soh, A. Atalar, and B. T. Khuri-Yakub, "Surface micromachined capacitive ultrasonic transducers," *IEEE Trans. Ultrason., Ferroelect., Freq. Contr.*, vol. 45, pp. 678–689, May 1998.

[17] B. Bayram, G. G. Yaralioglu, A. S. Ergun, Ö. Oralkan, and B. T. Khuri-Yakub, "Dynamic FEM analysis of multiple cMUT cells in immersion," in *Proc. IEEE Ultrason. Symp.*, 2004, pp. 252–255.

[18] B. Bayram, G. G. Yaralioglu, M. Kupnik, A. S. Ergun, Ö. Oralkan, A. Nikoozadeh, and B. T. Khuri-Yakub, "Dynamic analysis of capacitive micromachined ultrasonic transducers," *IEEE Trans. Ultrason., Ferroelect., Freq. Contr.*, vol. 52, no. 12, pp. 2270–2275, Dec. 2005.

[19] C.-P. Chang, "MEMS for telecommunications: Devices and reliability," in *Proc. Custom Integrated Circuits Conf.*, 2003, pp. 199–206.

[20] E. K. Chan, K. Garikipati, and R. W. Dutton, "Characterization of contact electromechanics through capacitance-voltage measurements and simulations," *IEEE/ASME J. Microelectromech. Syst.*, vol. 8, no. 9, pp. 208–217, June 1999.

[21] A. Y. Suh and A. A. Polycarpou, "Adhesion and pull-off forces for polysilicon MEMS surfaces using the sub-boundary lubrication model," *ASME J. Tribol.*, vol. 125, pp. 193–199, Jan. 2003.

[22] J. R. Reid and R. T. Webster, "Measurements of charging in capacitive microelectromechanical switches," *Electron. Lett.*, vol. 38, no. 24, pp. 1544–1545, 2002.

[23] J. R. Reid, R. T. Webster, and L. A. Starman, "Noncontact measurement of charge induced voltage shift in capacitive MEMswitches," *IEEE Microwave Wireless Comp. Lett.*, vol. 13, no. 9, pp. 367–369, Sep. 2003.

[24] Y. Huang, E. Hæggström, X. Zhuang, A. S. Ergun, and B. T. Khuri-Yakub, "A solution to the charging problems in capacitive micromachined ultrasonic transducers," *IEEE Trans. Ultrason., Ferroelect., Freq. Contr.*, vol. 52, no. 4, pp. 578–580, Apr. 2005.

**Ömer Oralkan** (S'93–M'05) received the B.S. degree from Bilkent University, Ankara, Turkey, in 1995, the M.S. degree from Clemson University, Clemson, SC, in 1997, and the Ph.D. degree from Stanford University, Stanford, CA, in 2004, all in electrical engineering.

Currently, he is an engineering research associate at the E. L. Ginzton Laboratory at Stanford University. His past and present research interests include analog and digital circuit design, micromachined sensors and actuators, and semiconductor device physics and fabrication. His current research focuses on the design and implementation of integrated ultrasonic imaging systems.

Dr. Oralkan received the 2002 Outstanding Paper Award of the IEEE Ultrasonics, Ferroelectrics, and Frequency Control Society. He is a member of the IEEE.

**Baris Bayram** (S'02) was born in Izmir, Turkey. He received the B.S. degree in 2000 from Bilkent University, Ankara, Turkey, the M.S. degree in 2002 from Stanford University, Stanford, CA, all in electrical engineering. He is currently a Ph.D. candidate in electrical engineering at the E. L. Ginzton Laboratory of Stanford University.

His current research interests include the accurate modeling of capacitive micromachined ultrasonic transducers (CMUTs) using static and dynamic finite element modeling. He particularly investigates the nonlinear operation regimes (collapsed and collapse-snapback) of CMUTs for high performance. He is a student member of the IEEE.

**Goksen G. Yaralioglu** (S'92–M'99) was born in Akhisar, Turkey, in 1970. He received his B.S., M.S., and Ph.D. degrees from Bilkent University, Ankara, Turkey, in 1992, 1994, and 1999, respectively, all in electrical engineering.

Currently, he is an engineering research associate in E. L. Ginzton Laboratory, Stanford University, Stanford, CA. His past and present research interests include design, modeling, and applications of micromachined ultrasonic transducers, atomic force microscopy at ultrasonic frequencies, and acoustic microscopy.

**A. Sanli Ergun** (S'91–M'99) was born in Ankara, Turkey, in 1969. He received his B.Sc., M.Sc., and Ph.D. degrees in 1991, 1994, and 1999, respectively, all in electrical and electronics engineering from Bilkent University, Ankara, Turkey.

He is now in E. L. Ginzton Laboratory, Stanford University, Stanford, CA, as an engineering research associate. His main research interests are acoustics, ultrasound, microelectromechanical systems (MEMS), and microwave electronics.

**Mario Kupnik** was born in Leoben, Austria, in 1974. He received his M.S. degree in electronics engineering from the Graz University of Technology, Graz, Austria, in 2000. From summer 1999 to October 2000, he worked as an analog design engineer for Infineon Technologies AG, Graz, Austria, on the design of ferroelectric memories and contactless smart card systems.

From 2000 to 2004, Dr. Kupnik worked as a research assistant at the Christian-Doppler Laboratory for Sensory Measurement, c/o Institute for Automation, University of Leoben, Leoben, Austria. He received his Ph.D. degree in physical measurement techniques from the University of Leoben in 2004 for his research in ultrasonic flow metering of hot gaseous mixtures, focusing especially on the exhaust gases of automotive combustion engines.

He is currently a postdoctoral researcher in the Khuri-Yakub Ultrasonics Group at the E. L. Ginzton Laboratory at Stanford University, Stanford, CA. His research interests include the design and application of capacitive micromachined ultrasonic transducers, focusing especially on ultrasonic transit-time gas flowmeters for hot and pulsating gases, and on ultrasonic nondestructive evaluation. Dr. Kupnik received the 2004 Fred-Margulies Award of the International Federation of Automatic Control (IFAC). He holds four patents in the fields of analog front-end circuits for contactless smart card systems and ultrasonic transit-time gas flowmeters.

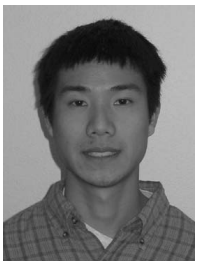

**David T. Yeh** (S'98) received the B.S. degree from the University of California at Berkeley in 2002, and the M.S. degree from Stanford University, Stanford, CA, in 2004, both in electrical engineering. He is currently pursuing a Ph.D. degree in electrical engineering at Stanford University.

He previously worked as an undergraduate researcher in the Berkeley Sensor and Actuator Center, Berkeley, CA, from 2000 to 2002 in MEMS research. In the summer of 2002 he worked at Hewlett-Packard Labs in Palo Alto, CA, characterizing thin film devices. In the summer of 2003 he performed research at National Semiconductor in Santa Clara, CA, on DC-DC power converters. From 2003 to 2005 he has been a graduate student in the Khuri-Yakub Ultrasonics Group at Stanford University. Currently he is a Ph.D. candidate in the Center for Computer Research in Music and Acoustics at Stanford University.

He is a member of IEEE. He received the National Defense Science and Engineering Graduate (NDSEG) fellowship and National Science Foundation (NSF) fellowship and was a student paper finalist at the 2005 Ultrasonics Symposium.

**Ira O. Wygant** (S'98) received his B.S. degree in electrical engineering with a cross-college major in computer science from the University of Wyoming, Laramie, WY, in 1999. He received his M.S. degree in electrical engineering from Stanford University, Stanford, CA, in 2002. He is currently pursuing a Ph.D. degree in electrical engineering at Stanford University.

He has held internships in the mixed-signal and monolithic sensors group at Oak Ridge National Laboratory, Oak Ridge, TN, in a wireless RF IC design group at Lucent Technologies, Reading, PA, and in the mixed-signal electronics group at Agilent Laboratories, Palo Alto, CA.

His research interests include IC and system design for ultrasound imaging systems based on capacitive micromachined ultrasonic transducers (CMUTs). He was the recipient of a National Science Foundation Graduate Research Fellowship.

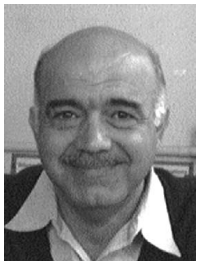

**Butrus T. Khuri-Yakub** (S'70–S'73–M'76–SM'87–F'95) was born in Beirut, Lebanon. He received the B.S. degree in 1970 from the American University of Beirut, Beirut, Lebanon, the M.S. degree in 1972 from Dartmouth College, Hanover, NH, and the Ph.D. degree in 1975 from Stanford University, Stanford, CA, all in electrical engineering. He joined the research staff at the E. L. Ginzton Laboratory of Stanford University in 1976 as a research associate. He was promoted to a senior research associate in 1978, and to a professor of electrical engineering (research) in 1982. He has served on many university committees in the School of Engineering and the Department of Electrical Engineering.

Presently, he is the Deputy Director of the E. L. Ginzton Laboratory. Dr. Khuri-Yakub has been teaching both at the graduate and undergraduate levels for over 15 years. His current research interests include in situ acoustic sensors (temperature, film thickness, resist cure, etc.) for monitoring and control of integrated circuits manufacturing processes, micromachining silicon to make acoustic materials and devices such as airborne and water immersion ultrasonic transducers and arrays, and fluid ejectors, and in the field of ultrasonic nondestructive evaluation and acoustic imaging and microscopy.

Dr. Khuri-Yakub is a fellow of the IEEE, a senior member of the Acoustical Society of America, and a member of Tau Beta Pi. He is associate editor of *Research in Nondestructive Evaluation*, a journal of the American Society for Nondestructive Testing. He has authored over 400 publications and has been principal inventor or co-inventor of 60 issued patents. He received the Stanford University School of Engineering Distinguished Advisor Award in June 1987 and the Medal of the City of Bordeaux for contributions to nondestructive evaluation, 1983.